RSC Advances

PAPER

View Article Online
View Journal | View Issue

Cite this: *RSC Adv.*, 2021, **11**, 16468

Molybdenum-modified mesoporous SiO_2 as an efficient Lewis acid catalyst for the acetylation of alcohols†

Xolani S. Hlatshwayo, Matumuene Joe Ndolomingo, Ndzondelelo Bingwa * and Reinout Meijboom *

A suitable, expeditious and well-organized approach for the acetylation of alcohols with acetic anhydride in the presence of 5%MoO_3–SiO_2 as an optimum environmentally benign heterogeneous catalyst was developed. The high surface area obtained for 5%MoO_3–SiO_2, 101 $m^2\ g^{-1}$ compared to other catalysts, 22, 23, and 44 $m^2\ g^{-1}$ for 5%WO_3–ZrO_2, 5%WO_3–SiO_2, and 5%MoO_3–ZrO_2, respectively, appears to be the driving force for better catalytic activity. Amongst the two dopants used, molybdenum oxide is the better dopant compared to its tungsten oxide counterpart. High yields of up to 86% were obtained with MoO_3 doping while WO_3 containing catalysts did not show any activity. Other reaction parameters such as reactor stirring speed, and solvent variation were studied and revealed that the optimum stirring speed is 400 rpm and cyclohexane is the best solvent. Thus, the utilization of affordable and nontoxic materials, short reaction times, reusability, and producibility of excellent yields of the desired products are the advantages of this procedure.

Received 17th March 2021
Accepted 26th April 2021

DOI: 10.1039/d1ra02134f

rsc.li/rsc-advances

1. Introduction

The acetylation of hydroxyl groups is a fundamental process that is frequently utilized in the transformation of organic compounds as it provides an alternative route that is affordable and efficient in organic synthesis.[1,2] In organic synthesis, the protection of functional groups is essential.[3] Thus, through the various transformations of functional groups, the protection of such functional groups that results in the acetylated species is highly important.[4] The obtained acetylated species can often be utilized in a range of ways such as through protection of functional groups in multistep synthetic processes.[5,6] Generally, the acetylated species are obtained from the most frequently utilized reagent combination which uses an acid anhydride in the presence of an acid[7–15] or base.[16–18] Furthermore, the acetylated groups are also more frequently found in pharmaceuticals, solvents, cosmetics, fragrances and foodstuffs as well as in plasticizers.[19,20]

Numerous methods for the acetylation reactions have been previously reported.[21–23] However, countless of these reported methods suffer from several limitations such as drastic reaction conditions, long reaction time, formation of toxic or undesirable byproducts, use of expensive reagents, utilization of catalysts which are moisture sensitive or toxic, tedious workup procedures and poor yields of the desired products.[5,21–25] Therefore, the developments of new catalysts and mild methods for the acetylation of alcohols are still in great demands. The transformation of various chemicals under heterogeneous catalysis has gained a great deal of interest over the past years due to the following findings; the efficiency of chemical transformations is greatly improved, improvement of the desired pure products, easier work-up, and usage of less toxic and affordable catalysts.[26,27]

In the recent years, there were some developments made to instigate solid reagents or solid reagents supports for uncomplicated work-ups which comprise silica gel supported $TaCl_5$,[28] $NaHSO_4$,[29] KSF,[30] Sc(III) or La(III) triflates.[31] Nonetheless, several of these catalysts contained some disadvantages like the production of unwanted byproducts, expeditious catalyst deactivation, and severe reaction conditions.[32] There are still some serious concerns with regards to green chemistry, hence numerous efforts of replacing ordinary catalysts with new solid acids that contain few advantages such as easily separable after the reaction, reusability, and presenting minimal toxicity are applied worldwide.[6,32] Thus, extensive exploitation of mesoporous metal oxides could be a breakthrough for the development of environmentally benign solid Lewis acid catalysts.[33]

Center for Synthesis and Catalysis, Department of Chemical Sciences, University of Johannesburg, P.O. Box 524, Auckland Park, 2006 Johannesburg, South Africa. E-mail: rmeijboom@uj.ac.za; Fax: +27 11 559 2819; Tel: +27 11 559 2367

† Electronic supplementary information (ESI) available: Scanning electron microscopy images (a) 5%WO_3–ZrO_2, (b) 5%MoO_3–SiO_2, (c) 5%MoO_3–ZrO_2, and (d) 5%WO_3–SiO_2 (Fig. S1). EDX spectrums of (a) 5%MoO_3–SiO_2, (b) 5%MoO_3–ZrO_2, (c) 5%WO_3–SiO_2, and (d) 5%WO_3–ZrO_2 (Fig. S2). NH_3-TPD of (a) 5%MoO_3–ZrO_2, (b) 5%WO_3–SiO_2, and (c) 5%WO_3–ZrO_2 (Fig. S3). TPR of the synthesized solid Lewis acid catalysts (Fig. S4). Thermogravimetric analysis and their derivatives: (a) 5%WO_3–SiO_2, (b) 5%WO_3–ZrO_2, and (c) 5%MoO_3–ZrO_2 (Fig. S5). See DOI: 10.1039/d1ra02134f

More recently, investigations revealed that molybdenum or tungsten doped zirconium is an alternative efficient catalyst essential for reactions requiring vigorous acid site.[34,35] Bearing this in mind, the development of well-organized effective green catalysts is still part of ongoing work.[36,37] Herein, we wish to report the use of 5%MoO_3–SiO_2 as an efficient solid acid catalyst for the acetylation of alcohols (Scheme 1) under mild reaction conditions.

2. Experimental

2.1. Materials

Ammonium metatungstate hydrate ($H_{26}N_6O_{40}W_{12}\cdot xH_2O$) (≥99.0%), ammonium molybdate tetrahydrate ($H_{24}Mo_7N_6O_{24}\cdot 4H_2O$) (81.0–83.0%), tetraethyl orthosilicate ($C_8H_{20}O_4Si$) (≥99.0%), zirconium(IV) oxynitrate hydrate ($N_2O_7Zr\cdot xH_2O$) (99%), decane ($C_{10}H_{22}$) (≥99%), dichloromethane (CH_2Cl_2) (≥99.8%), nitric acid (HNO_3) (70%), geraniol ($C_{10}H_{18}O$) (98%), ethylene glycol ($C_2H_6O_2$) (99.8%), 2-phenylethanol ($C_8H_{10}O$) (≥99.0%), 3-phenyl-2-propyn-1-ol (C_9H_8O) (96%), and poly(-ethylene glycol)-*block*-poly(propylene glycol)-*block*-poly(ethylene glycol), nonyl acetate ($C_{11}H_{22}O_2$) (≥97.0%), pentyl acetate ($CH_3COO(CH_2)_4CH_3$) (99.0%), 2-phenethyl acetate ($CH_3COOCH_2CH_2C_6H_5$) (≥99.0%), benzyl acetate ($CH_3COOCH_2C_6H_5$) (≥99.0%), hexyl acetate ($CH_3COO(CH_2)_5CH_3$) (99.0%), *sec*-butyl acetate ($CH_3CO_2CH(CH_3)C_2H_5$) (99.0%), *tert*-butyl acetate ($CH_3COOC(CH_3)_3$) (≥99.0%), and geranyl acetate ($CH_3CO_2CH_2CH{=}C(CH_3)CH_2CH_2CH{=}C(CH_3)_2$) (≥97.0%) were all purchased from Sigma Aldrich. Toluene ($C_6H_5CH_3$) (99.8%) and cyclohexane ($C_{10}H_{12}$) (98%) were purchased from Rochelle Chemicals. Acetic anhydride [$(CH_3CO)_2O$] (97%) was purchased from UniLAB. All chemicals were used as received.

2.2. Catalyst synthesis

The solid acid catalysts were synthesized by the sol–gel method as described by Poyraz *et al.*,[38] following the approach of Corma.[39] 430 μmol of P123 and 0.02 mol of each metal precursor were added into two separate 300 mL beaker, and then 0.19 mol of *n*-butanol and 0.04 mol of HNO_3 were added to the mixtures. The mixtures were stirred at 25 °C until transparent gels were acquired. Two other mixtures of 0.001 mol of ammonium molybdate and ammonium metatungstate were separately prepared in 300 mL beakers. Thus, each salt was added inside a stirring beaker which contained 2.5 g of Milli-Q water plus 2.5 g of ethanol. As soon as the salt solution became clear, it was transferred into the acquired clear gel under vigorous stirring, and the mixture was further stirred vigorously for 20 minutes. The amounts added of both molybdenum and tungsten were 5 mol% (molX/molY × 100, where X = MoO_3 or WO_3 and Y = ZrO_2 or SiO_2). The obtained mixture was placed inside an oven set at 120 °C for six hours and immediately calcined for 1 hour at 600 °C under air. The generated brittle materials were crushed and marked 5%X–Y.

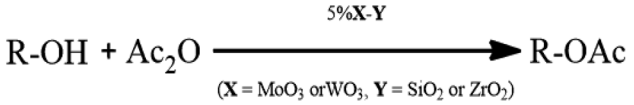

Scheme 1 Catalytic acetylation of alcohols with acetic anhydride.

2.3. Instrumentation

Prior to nitrogen sorption experiments (BET analysis) on Micromeritics ASAP 2460 surface area and porosity analyzer at −196 °C, the acquired powder samples were degassed under nitrogen gas for 8 hours at 90 °C and further degassed under vacuum at 250 °C for another 8 hours. A Rigaku MiniFlex-600 diffractometer with Cu Kα radiation (λ = 1.5406 Å) was utilized at room temperature for carrying out analysis of wide and low-angle powder X-ray diffraction (p-XRD). SDT Q600 thermogravimetric analyzer (TGA) was utilized to scrutinize the thermal behavior of our prepared catalysts under nitrogen flow, with a range of 10 °C min^{-1} from 30 to 1000 °C. Samples were firstly carbon-coated using an Agar Turbo Carbon Coater and then analyzed Tescan Vega 3LMH Scanning Electron Microscopy (SEM) for imaging, morphology and elemental mapping. JEOL JEM-2100F electron microscope consisting of 200 kV accelerating voltage was used to capture Transmission Electron Microscopy (TEM) images of our synthesized catalysts for the estimation of the particle sizes. The acid sites of the as synthesized catalysts were verified by temperature programed desorption method (TPD) using a Chemisorption Analyzer Micromeritics AutoChem II 2920. The Carousel 12 plus reaction station from Radleys TECH was utilized for monitoring the stirring speed and the temperature of the reactions. For qualitative analysis, Shimadzu GC-MS equipped with the mass selective detector and the capillary column was utilized for the qualitative analysis. Shimadzu GC-2010 equipped with Restek-800-356-1688 capillary column (30 m × 0.25 mm × 0.25 μm) and flame ionization detector (FID) was utilized for quantitative analysis. Temperatures of 250 °C and 300 °C were utilized for FID and injection port respectively. For the separation process during catalyst recycling, a NEYA 8 benchtop centrifuge was successfully utilized.

2.4. Catalytic evaluation

To a solution of alcohol (2 mmol) and acetic anhydride (3 mmol), 5%X–Y (X = MoO_3 or WO_3, Y = ZrO_2 or SiO_2) was added. The reaction solution was stirred (400 rpm) at 35 °C for 30 minutes and consecutively sampled after every 5 minutes. Thus, the reaction progress was monitored by GC. The controlled experiments revealed that no reaction took place in the absence of the catalyst and the tungsten promoter was inactive in this reaction. The results showed that the reaction is favorable towards MoO_3 as the catalyst promoter. 5%MoO_3–SiO_2 was revealed to be an ideally suited solid acid catalyst for the acetylation of alcohols. For catalyst recyclability, the optimum catalyst (30 mg) was transferred into a Falcon tube (500 mL) and thoroughly washed three times with cyclohexane (15 mL). After each wash, the solution was centrifuged at 4500 rpm for 15 minutes.

3. Results and discussions

3.1. Synthesis and characterization

Thermally stable solid Lewis acid catalysts were synthesized by the sol–gel method described by Poyraz *et al.*[38] Due to the presence of nitrate ions, color changes such as molybdenum solution turning dark yellow and tungsten solution becoming opaque were observed. This is in agreement with the report in the literature.[40] The acquired parameters such as surface areas, pore diameters, pore volumes, acidic sites, and crystallite sizes are summarized in Table 1. Nitrogen sorption analysis confirmed that the prepared materials were within mesoporous materials range of 2–50 nm. Mesoporous metal oxides have remarkable features like high surface areas, easily tunable, chemical and thermal stability. Generally, materials with higher surface areas turn to be more active and become favorable for most reactions.[41,42] Looking at 5%MoO_3–Y catalysts on Table 1, it was observed that SiO_2 gave higher surface area (100.8 $m^2\ g^{-1}$) compared to ZrO_2 (44.1 $m^2\ g^{-1}$). There is no clear correlation between the surface area these materials possess and the acidic sites on their surface.

As shown in Fig. 1(a), nitrogen sorption of the synthesized solid Lewis acid catalysts aged at 600 °C conveyed type IV isotherms with hysteresis loop associated with capillary condensation taking place in the mesopores, confirming the mesoporosity of the as-synthesized materials.[43,44] Fig. 1(b)

Table 1 BET, XRD and TPD characterization of the solid Lewis acid catalysts

Catalyst	A_{BET} ($m^2\ g^{-1}$)	P_v ($cm^3\ g^{-1}$)	P_D (nm)	Crystallite size (nm)	Acidic sites (a.u.)
5%MoO_3–SiO_2	101	0.29	11.6	104.9	0.05
5%MoO_3–ZrO_2	44	0.13	11.7	14.5	0.03
5%WO_3–SiO_2	23	0.02	3.7	8.1	0.04
5%WO_3–ZrO_2	22	0.07	12.8	37.7	0.06

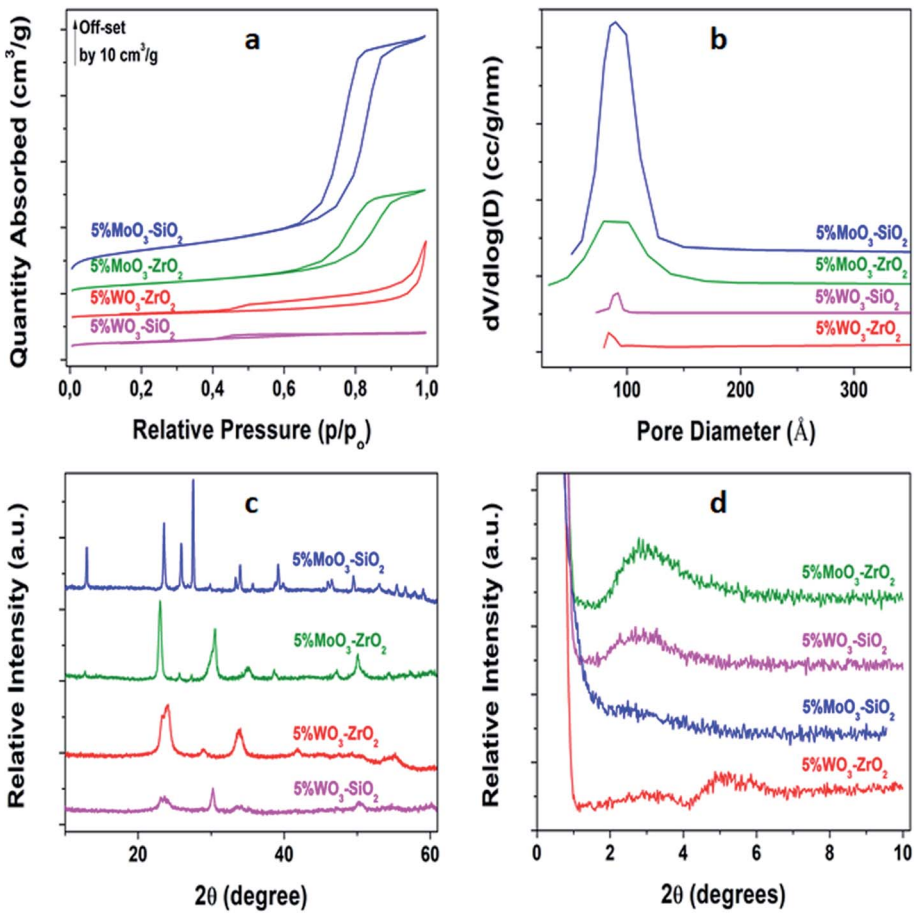

Fig. 1 Characterization of the synthesized MMO's (a) BET N_2-sorption isotherms, (b) BJH desorption pore volume distribution, (c) wide-angle p-XRD, and (d) low-angle p-XRD.

depicts the corresponding pore size distributions, acquired from utilizing BJH calculation procedure. It can be observed that the MoO_3-based catalysts have wide pore size distribution, while the WO_3-based catalysts possess narrow pore size distribution of uniform size. X-ray diffraction patterns of the synthesized solid Lewis acid catalysts calcined at 600 °C are displayed in Fig. 1(c). Moreover, for MoO_3 doping shaper peaks were observed indicating non-crystalline characteristic of 5% MoO–SiO_2 and 5%MoO_3–ZrO_2 catalysts. However, the WO_3 promoter revealed broad peaks because of the amorphous nature of 5%WO_3–SiO_2 and 5%WO_3–ZrO_2 catalysts. As shown in Fig. 1(d), all the synthesized mesoporous metal oxides catalysts except 5%MoO_3–SiO_2 exhibited diffraction peaks at low angles. The 5%MoO_3–SiO_2 depicted broad peak-like characteristic which was unclear due to low intensity indicating that the obtained pores did not indicate the regular mesostructured.[45]

As illustrated in Fig. 2, TEM images provided some insights into mesopore structural features. These acquired images illustrated the arrangement of crystallite which clearly indicated that pores were present. Thus, it was observed that upon using molybdenum as a promoter intensified the thermal stability and also enhanced the surface areas as shown in Table 1. However, utilizing tungsten as a promoter resulted in the amorphous materials which had dark spots that were previously ascribed to tungsten clusters from the literature.[46,47] Fig. S1† shows the representative SEM images of the calcined mesoporous metal oxides. Moreover, a closer inspection of the synthesized materials revealed that they contained uneven surfaces with countless pores irregularly shaped. Thus, the EDX analysis conducted (Fig. S2†) confirmed that no impurities were present in our synthesized mesoporous metal oxides catalysts.

In most cases, the acidity of mesoporous metal oxides plays an essential role in numerous reactions. Consequently, the acidity of mesoporous metal oxides needs to be investigated. The properties of solid acids also consist of strength, type, and a number of acid sites. Thus, NH_3-TPD is an ideal method which is utilized extensively for determining the active site on a catalyst.[48,49] Fig. 3(a) depicts peak areas of 5%MoO_3–SiO_2. It was clearly observed that elevating the heating rate from 5 to 20 °C min^{-1} resulted in the increment of the peak areas, where the peak area is equivalent to the active site. For all the synthesized catalysts it was observed that the heating rates were directly proportional to the peak areas (see Fig. S3†). Thus, TPR experiments were conducted to acquire a deep understanding of the synthesized mesoporous metal oxides.

Fig. S4† shows the acquired profiles which exhibit multiple reduction peaks. Looking at molybdenum promoter, it was previously reported that it had two peaks at 767 and 997 °C,

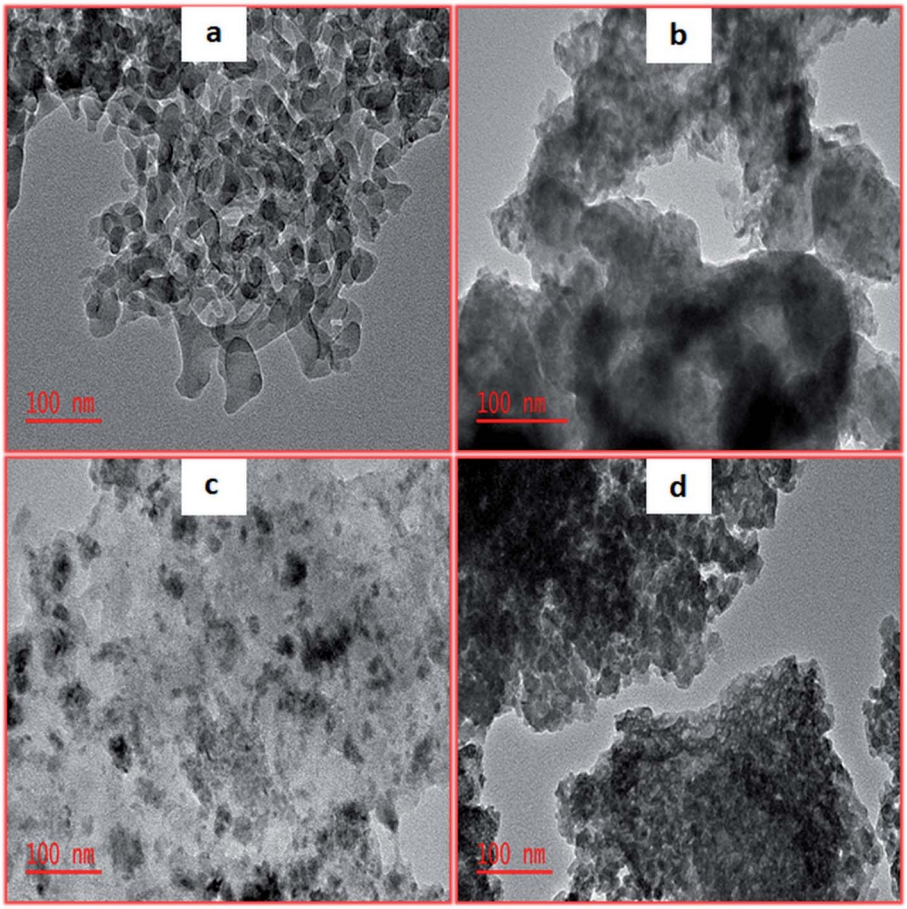

Fig. 2 TEM images of (a) 5%MoO_3–SiO_2, (b) 5%WO_3–ZrO_2, (c) 5%WO_3–SiO_2 and (d) 5%MoO_3–ZrO_2.

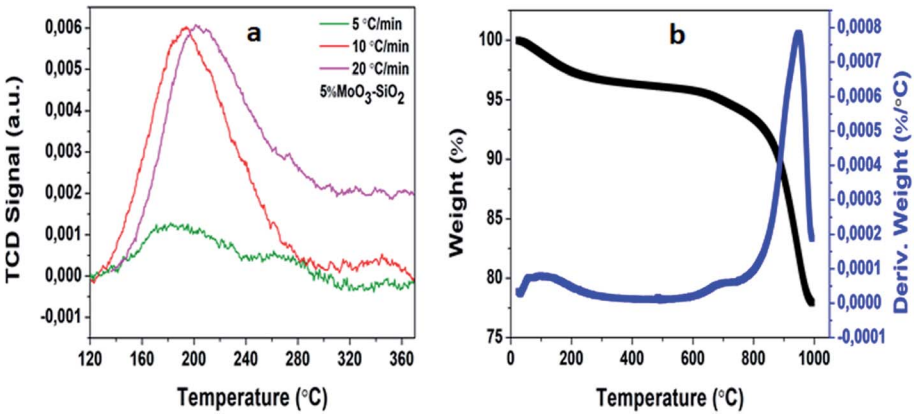

Fig. 3 The depiction of 5%MoO_3–SiO_2 *via* (a) NH_3-TPD and (b) thermogravimetric analysis and its derivative.

respectively.[49] Furthermore, it was observed that upon promoting silica and zirconium, the reduction peaks migrated to lower temperatures, demonstrating excessive reducibility.[50] Generally, tungsten undergoes three reduction steps as previously reported.[51] The obtained results of 5%WO_3–Y only revealed two reduction peaks shifted to lower temperatures instead of three possible peaks which might be due to the limitation of temperature range on the instrument used. Fig. 3(b) depicts the thermogravimetric analysis curve of 5% MoO_3–SiO_2 and its derivation curve. For this optimum catalyst, it was observed that three decomposition steps took place. The dehydroxylation[52] from 50 up to 73 °C, followed by the weight

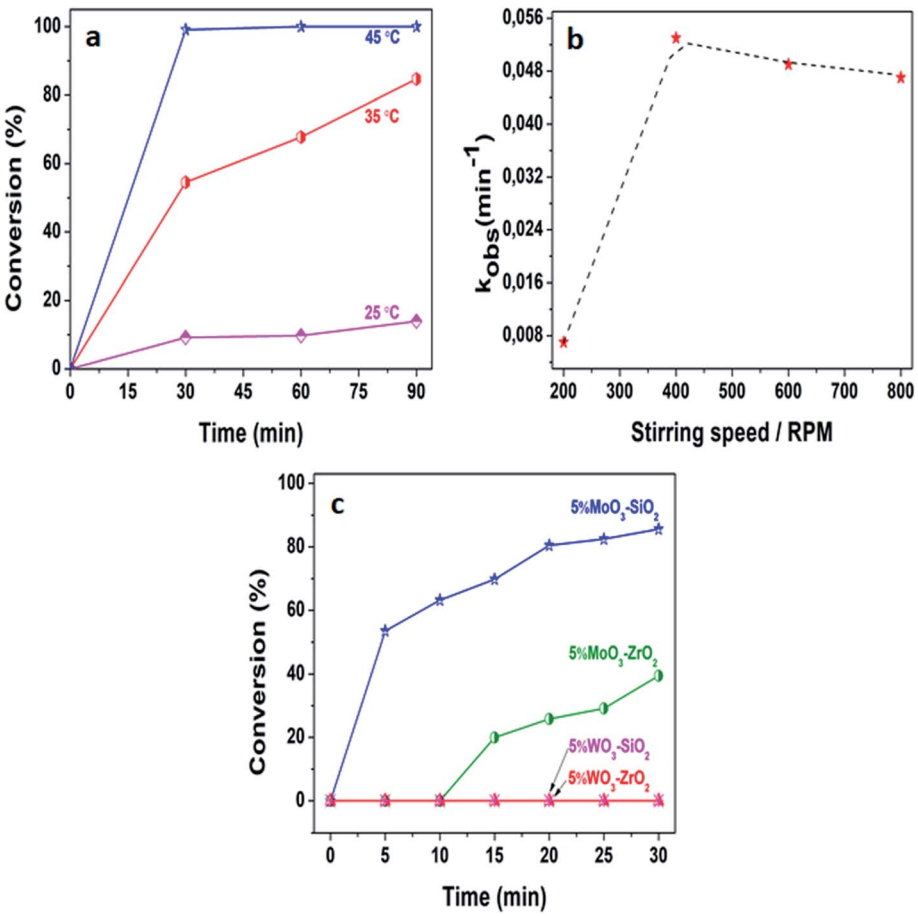

Fig. 4 (a) The effect of temperature upon the acetylation of 2-phenylethanol, (b) the influence of stirring speed at 35 °C, and (c) performance of different catalysts at 35 °C and 400 rpm. The reaction conditions were: acetic anhydride = 3 mmol, toluene = 6 mL, decane = 0.132 mmol, 2-phenylethanol = 2 mmol, and catalyst amount = 25 mg.

loss at 734 °C, and the third decomposition at 948 °C corresponding to the detachment of oxygen molecules.[53] The total weight loss observed for this specific catalyst was 23 wt%. The rest of the synthesized solid Lewis acid catalysts are shown in Fig. S5† with 5%MoO_3–ZrO_2 exhibiting the average weight loss of 2.75 wt%, 5%WO_3–SiO_2 revealing the average weight loss of 24 wt%, and lastly, 5%WO_3–ZrO_2 depicting the average weight loss of about 18.5 wt%.

3.2. Optimization of the catalytic variables

Generally, the exploitation of mesoporous metal oxides is considered as one of the promising developments of the desired solid Lewis acid catalysts which are environmentally friendly and suitable for a variety of sustainable chemistry.[33] Herein, we delineate a mild, convenient and efficient approach for the acetylation of various alcohols that is typically performed utilizing acetic anhydride in the presence of solid Lewis acid catalysts. To maximize the desired yields, the reaction conditions were firstly optimized. We investigated the capability of 5%MoO_3–SiO_2 in the acetylation of 2-phenylethanol, in which an insignificant activity was acquired at room temperature, whereby toluene was utilized as a solvent. Thus, certain parameters such as temperatures, stirring speeds, solvents, substrates, and catalyst amount were intensely investigated in order to enhance the activity and the producibility of the desired products. Fig. 4(a) demonstrate the impact of distinct temperatures on the acetylation of 2-phenylethanol. It was clearly illustrated that the reaction temperature is directly proportional to the activity. Thus, after establishing the optimum temperature of 35 °C, the stirring speed was also investigated as illustrated in Fig. 4(b). It was clearly observed that the diffusion zone whereby the reaction was independent of the stirring speed appeared after 400 rpm, hence we deduced that the optimum stirring speed for further investigation was 400 rpm. Fig. 4(c) depicts the activity of different catalysts with 5%MoO_3–SiO_2 being the most favourable catalyst for the acetylation of 2-phenylethanol. This is a result of the high surface area this catalyst possess coupled with the fairly acceptable acidity, see Table 1. No activity was observed upon using 5%WO_3–Y catalysts, indicating that the tungsten promoter was inactive towards this specific reaction. The reaction was also performed with similar reaction parameters to investigate the formation of the product in the absence of the catalyst and it was observed that no traces

Table 2 Comparison of the effectiveness of 5%MoO_3–SiO_2 with other catalysts for the acetylation of 2-phenylethanol[a]

Catalyst	Temp. (°C)	Time (min)	Yield (%)	Solvent	Ref.
5%MoO_3–SiO_2	35	30	86	Toluene	TW
5%MoO_3–ZrO_2	35	30	40	Toluene	TW
5%WO_3–SiO_2	35	30	—	Toluene	TW
5%WO_3–ZrO_2	35	30	—	Toluene	TW
Catalyst-free	35	30	—	Toluene	TW
$H_{14}[NaP_5W_{30}O_{110}]$	25	90	95	Solvent-free	54
Cp_2ZrCl_2	25	840	90	Solvent-free	55
Fluorous distannoxane	25	360	72	Toluene	56
1,3-Dibromo-5,5-dimethylhydantoin	25	1800	90	Dichloromethane	57

[a] TW: this work.

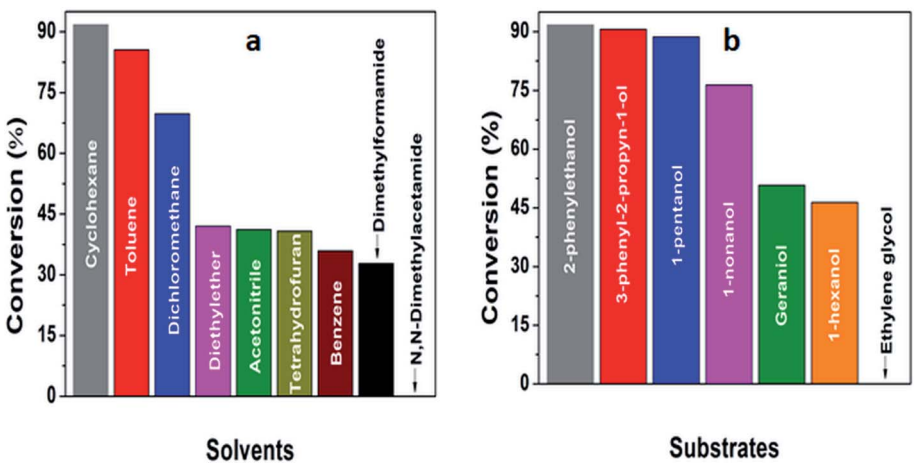

Fig. 5 (a) The investigation of an effective solvent, (b) deducing an optimum substrate for further investigation. The reaction conditions were: solvents = 6 mL, decane = 0.132 mmol, acetic anhydride = 3 mmol, substrates = 2 mmol, stirring speed = 400 rpm, and catalyst amount = 25 mg.

of the product were acquired from the GC analysis. Furthermore, we compared these obtained results with literature as noted in Table 2. It follows that most reported catalysts such as fluorous distannoxane[56] required longer reaction time for the acetylation of 2-phenylethanol and gave lower yield. Thus, 5% MoO_3–SiO_2 afforded great catalytic improvement on the acetylation of alcohols under mild reaction conditions, hence it was considered as an efficient Lewis acid catalyst. Interestingly, 86% of 2-phenylethanol was converted within 30 minutes under mild reaction condition.

The ability of 5%MoO_3–SiO_2 catalyst was investigated on several solvents as illustrated in Fig. 5(a). Cyclohexane was revealed to be the best solvent, followed by toluene and dichloromethane, while the use of *N*,*N*-dimethylacetamide as solvent did not display any conversion. Thus, the choice of an appropriate solvent is crucial for the efficiency of the study reaction. Consequently, cyclohexane which afforded the yield of 91.8% was deduced as the optimum solvent for further investigation. Later, a variety of substrates was investigated under the same reaction conditions using cyclohexane as solvent. It was observed that the best yield (91.8%) was obtained when 2-phenylethanol was used as substrate, followed by 3-phenyl-2-propyn-1-ol with a yield of 90.6% (see Fig. 5(b) and Table 3). Furthermore, it is noteworthy that secondary and tertiary alcohols such as 2-butanol and *tert*-butanol (entry 9 and 10, Table 3) can be acetylated indicating that the catalyst was not only limited to primary alcohols. Additionally, we investigated the impact of the mass transfer limitation whereby a variety of catalyst amounts were utilized as illustrated in Fig. 6(a). The data presented in Fig. 6(a), the change in concentration of the

Table 3 Acetylation of selected alcohols with acetic anhydride over 5%MoO_3–SiO_2 under mild reaction conditions

Entry[a]	Substrate	Product[b]	Yield (%)
1	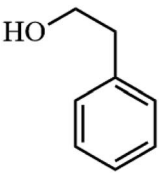	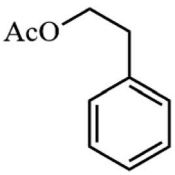	91.8
2	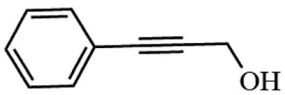	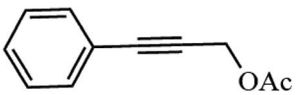	90.6
3	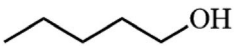		88.6
4	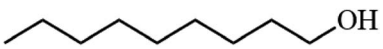	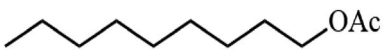	76.4
5	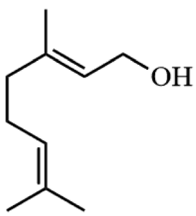	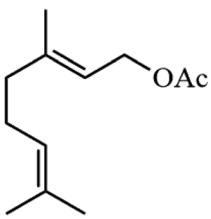	50.8
6	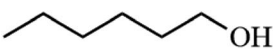	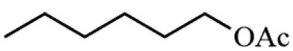	46.4
7	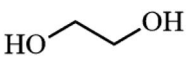	—	—
8	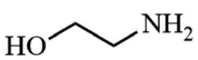	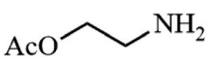	86.9
9	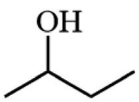	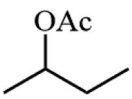	65.4
10	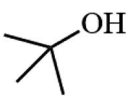	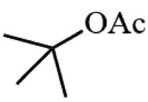	31.7

[a] Reaction conditions: substrate = 2 mmol, Ac_2O = 3 mmol, cyclohexane = 0.056 mol, 5%MoO_3–SiO_2 = 25 mg, temperature = 35 °C, time = 30 min.
[b] Products: they were all confirmed with GC-MS and the standards were used as well.

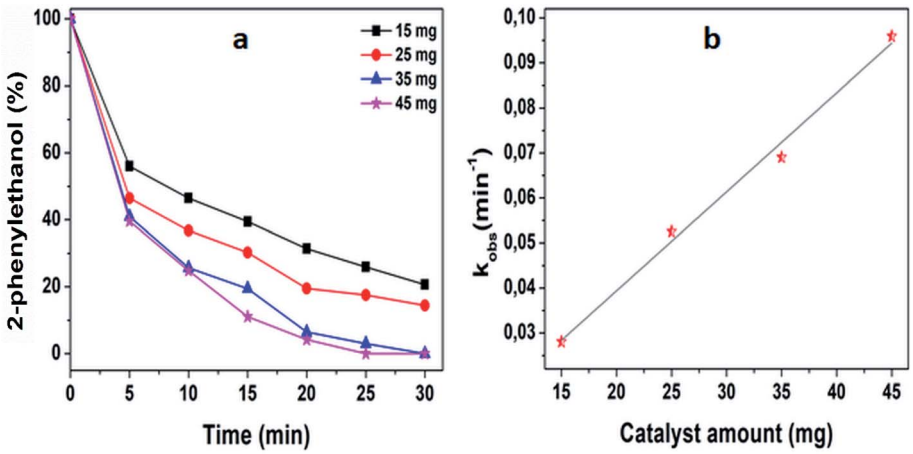

Fig. 6 (a) Various amount of optimum catalyst, (b) the study of mass transfer limits. The reaction conditions were: cyclohexane = 6 mL, decane = 0.132 mmol, acetic anhydride = 3 mmol, 2-phenylethanol = 2 mmol, stirring speed = 400 rpm, and catalyst amount = 25 mg.

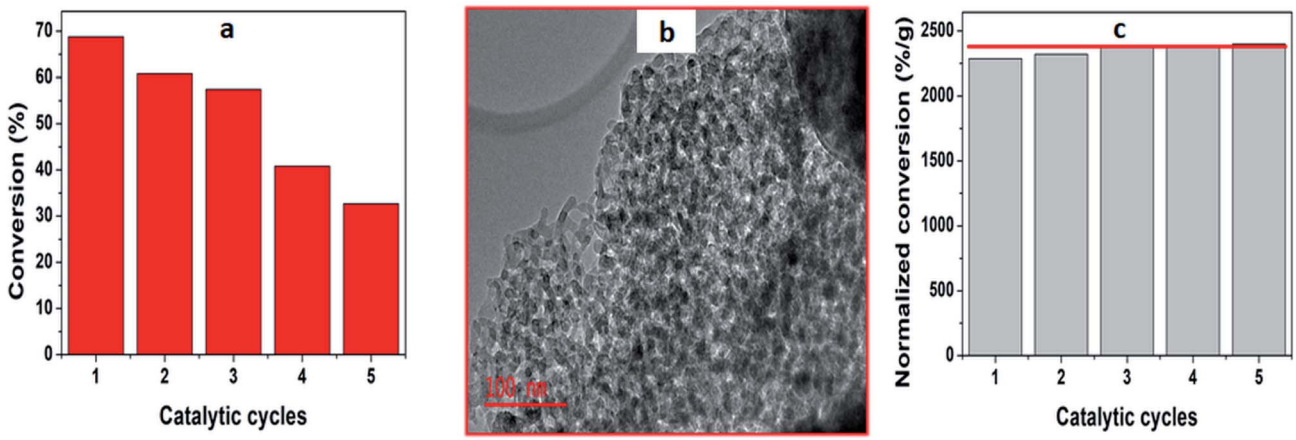

Fig. 7 (a) The catalytic recycle test of the optimum catalyst, (b) TEM image and (c) the normalized by mass conversion. Reaction conditions: 6 mL of cyclohexane, temperature = 35 °C, decane = 0.132 mmol, acetic anhydride = 3 mmol, 2-phenylethanol = 2 mmol, stirring speed = 400 rpm.

substrate with time was used to study the kinetics of the reaction. It is clear from Fig. 6(b) that the rate of conversion of the substrate increases with increase in the catalysts surface area available in the reactor. From these findings, as depicted in Fig. 6(b) it can be deduced that the mass transport limitation did not affect any conversion. The initial rate was directly proportional to the catalyst amount, and the linear increasing confirmed the absence of the mass transfer limitation.

3.3. Catalyst recyclability

Moreover, after deducing the kinetic zone, it follows that we took 30 mg of the catalyst which was within the kinetic zone for the catalyst recycling tests. Fig. 7 illustrates the reusability of 5% MoO_3–SiO_2 on the acetylation of 2-phenylethanol up to the fifth run from Fig. 7(a), it can be observed that the catalyst was recyclable but the activity decreases as the number of reaction cycles increases. This is due to some loss of the catalyst during the separation process between each recycling test. However, to confirm the stability of the catalyst, the conversion was normalized by the amount of catalyst used in each reaction cycle, and it was observed that the catalyst was very stable with only minor loss in activity (Fig. 7(c)). TEM analysis was performed after the 5th catalytic cycle and it was observed that the mesostructure of the catalyst was not affected as illustrated in Fig. 7(b). The stability of the catalysts could be due to the stable structure of the as-synthesized materials, and this feature could make them good catalysts for industrial application.

4. Conclusion

In conclusion, highly stable meso-structured solid acid nanocatalysts such as 5%MoO_3–SiO_2 can be synthesized using a sol–gel method. We have demonstrated that 5%MoO_3–SiO_2 is a flexible and very effective inexpensive heterogeneous catalyst for the acetylation of alcohols with acetic anhydride. The results show that the as-synthesized catalyst was highly selective towards the desired products. The notable advantages of this catalyst are the producibility of excellent yields, shorter reaction

times, and lower reaction temperatures. Also, the catalyst was revealed to be environmentally friendly and could be reused a number of times without loss of activity and selectivity.

Conflicts of interest

The authors declare no competing financial interest.

Acknowledgements

We acknowledge the financial support from South African NRF (Grant specific number 117997 and 111710), Analytical division (spectrum), Sasol R&D and research fund from the University of Johannesburg. We would also like to acknowledge Mr D. Hariss and Dr R. Meyer from Shimadzu South Africa for the usage of their equipment throughout this study.

References

1 T. W. Greene and P. G. M. Wuts, *Protective groups in organic synthesis*, Wiley, 1999.
2 P. J. Kocienski, *Protecting groups*, Thieme, Stuttgart, 1994, vol. 1.
3 T. W. Green and P. G. M. Wuts, *Protective Groups in Organic Synthesis*, New York, 1999, vol. 27, pp. 708–711.
4 M. Moghadam, S. Tangestaninejad, V. Mirkhani, I. Mohammadpoor-Baltork and S. A. Taghavi, *J. Mol. Catal. A: Chem.*, 2007, **274**, 217–223.
5 B. Das and P. Thirupathi, *J. Mol. Catal. A: Chem.*, 2007, **269**, 12–16.
6 L. Ma, I. Jia, X. Guo and L. Xiang, *Chin. J. Catal.*, 2014, **35**, 108–119.
7 T. Mukaiyama, I. Shiina and M. Miyashita, *Chem. Lett.*, 1992, **21**, 625–628.
8 K. Ishihara, M. Kubota, H. Kurihara and H. Yamamoto, *J. Org. Chem.*, 1996, **61**, 4560–4567.
9 A. Orita, C. Tanahashi, A. Kakuda and J. Otera, *Angew. Chem., Int. Ed.*, 2000, **39**, 2877–2879.
10 B. Karimi and J. Maleki, *J. Org. Chem.*, 2003, **68**, 4951–4954.
11 R. Dalpozzo, A. De Nino, L. Maiuolo, A. Procopio, M. Nardi, G. Bartoli and R. Romeo, *Tetrahedron Lett.*, 2003, **44**, 5621–5624.
12 S. Velusamy, S. Borpuzari and T. Punniyamurthy, *Tetrahedron*, 2005, **61**, 2011–2015.
13 T. S. Reddy, M. Narasimhulu, N. Suryakiran, K. C. Mahesh, K. Ashalatha and Y. Venkateswarlu, *Tetrahedron Lett.*, 2006, **47**, 6825–6829.
14 N. Ahmed and J. E. van Lier, *Tetrahedron Lett.*, 2006, **47**, 5345–5349.
15 A. Kamal, M. N. A. Khan, K. S. Reddy, Y. V. V. Srikanth and T. Krishnaji, *Tetrahedron Lett.*, 2007, **48**, 3813–3818.
16 W. Steglich and G. Höfle, *Angew. Chem., Int. Ed. Engl.*, 1969, **8**, 981.
17 E. F. V. Scriven, *Chem. Soc. Rev.*, 1983, **12**, 129–161.
18 E. Vedejs and S. T. Diver, *J. Am. Chem. Soc.*, 1993, **115**, 3358–3359.
19 H.-J. Yoon, S.-M. Lee, J.-H. Kim, H.-J. Cho, J.-W. Choi, S.-H. Lee and Y.-S. Lee, *Tetrahedron Lett.*, 2008, **49**, 3165–3171.
20 S. A. Taghavi, M. Moghadam, I. Mohammadpoor-Baltork, S. Tangestaninejad, V. Mirkhani and A. R. Khosropour, *Inorg. Chim. Acta*, 2011, **377**, 159–164.
21 A. Kamal, M. N. A. Khan, K. S. Reddy, Y. V. V. Srikanth and T. Krishnaji, *Tetrahedron Lett.*, 2007, **48**, 3813–3818.
22 V. Mirkhani, S. Tangestaninejad, M. Moghadam, B. Yadollahi and L. Alipanah, *Monatsh. Chem.*, 2004, **135**, 1257–1263.
23 F. Rajabi, *Tetrahedron Lett.*, 2009, **50**, 395–397.
24 F. Shirini, M. A. Zolfigol and M. Abedini, *Monatsh. Chem.*, 2004, **135**, 279–282.
25 J. R. Satam and R. V. Jayaram, *Catal. Commun.*, 2008, **9**, 2365–2370.
26 P. Laszlo, *Acc. Chem. Res.*, 1986, **19**, 121–127.
27 F. Bigi, S. Carloni, R. Maggi, C. Muchetti and G. Sartori, *J. Org. Chem.*, 1997, **62**, 7024–7027.
28 S. Chandrasekhar, T. Ramachander and M. Takhi, *Tetrahedron Lett.*, 1998, **39**, 3263–3266.
29 G. W. Breton, *J. Org. Chem.*, 1997, **62**, 8952–8954.
30 A. Arienti, F. Bigi, R. Maggi, E. Marzi, P. Moggi, M. Rastelli, G. Sartori and F. Tarantola, *Tetrahedron*, 1997, **53**, 3795–3804.
31 A. G. M. Barrett and D. C. Braddock, *Chem. Commun.*, 1997, 351–352.
32 B. M. Reddy and P. M. Sreekanth, *Synth. Commun.*, 2002, **32**, 2815–2819.
33 B. Tang, W. Dai, G. Wu, N. Guan, L. Li and M. Hunger, *ACS Catal.*, 2014, **4**, 2801–2810.
34 M. Hino and K. Arata, *Appl. Catal., A*, 1998, **169**, 151–155.
35 B. M. Reddy and V. R. Reddy, *Synth. Commun.*, 1999, **29**, 2789–2794.
36 A. R. Hajipour and G. Azizi, *Green Chem.*, 2013, **15**, 1030–1034.
37 A. R. Hajipour and H. Karimi, *Appl. Catal., A*, 2014, **482**, 99–107.
38 A. S. Poyraz, C.-H. Kuo, E. Kim, Y. Meng, M. S. Seraji and S. L. Suib, *Chem. Mater.*, 2014, **26**, 2803–2813.
39 A. Corma, A. Martinez and C. Martinez, *Appl. Catal., A*, 1996, **144**, 249–268.
40 N. Masunga, G. S. Tito and R. Meijboom, *Appl. Catal., A*, 2018, **552**, 154–167.
41 J. Xu, A. Zheng, J. Yang, Y. Su, J. Wang and D. Zeng, *J. Phys. Chem. B*, 2006, **110**, 10662–10671.
42 R. G. Pearson and J. Songstad, *J. Am. Chem. Soc.*, 1967, **39**, 1827–1836.
43 K. S. W. Sing, *J. Porous Mater.*, 1995, **2**, 5–8.
44 S. Storck, H. Bretinger and W. F. Maier, *Appl. Catal., A*, 1998, **174**, 137–146.
45 J. R. Matos, M. Kruk, L. P. Mercuri, M. Jaroniec, L. Zhao, T. Kamiyama, O. Terasaki, T. J. Pinnavaia and Y. Liu, *J. Am. Chem. Soc.*, 2003, **125**, 821–829.
46 W. Zhou, N. Soultanidis, H. Xu, M. S. Wong, M. Neurock, C. J. Kiely and I. E. Wachs, *ACS Catal.*, 2017, **7**, 2181–2198.

47 T. Yamamoto, A. Teramachi, A. Orita, A. Kurimoto, T. Motoi and T. Tanaka, *J. Phys. Chem. C*, 2016, **120**, 19705–19713.
48 A. Corma, *Chem. Rev.*, 1997, **97**, 2373–2420.
49 L. Damjanović and A. Auroux, in *Zeolite characterization and catalysis*, Springer, 2009, pp. 107–167.
50 W. Shan, W. Shen and C. Li, *Chem. Mater.*, 2003, **15**, 4761–4767.
51 D. C. Vermaire and P. C. Van Berge, *J. Catal.*, 1989, **116**, 309–317.
52 M. J. Ndolomingo and R. Meijboom, *Appl. Surf. Sci.*, 2016, **390**, 224–235.
53 X. Shen, A. M. Morey, J. Liu, Y. Ding, J. Cai, J. Durand, Q. Wang, W. Wen, W. A. Hines, J. C. Hanson, J. Bai, A. I. Frenkel, W. Rei, M. Aindow and S. L. Suib, *J. Phys. Chem. C*, 2011, **115**, 21610–21619.
54 M. M. Heravi, F. K. Behbahani and F. F. Bamoharram, *J. Mol. Catal. A: Chem.*, 2006, **253**, 16–19.
55 M. Lakshmi Kantam, K. Aziz and P. R. Likhar, *Catal. Commun.*, 2006, **7**, 484–487.
56 Z. Peng, A. Orita, D. An and J. Otera, *Tetrahedron Lett.*, 2005, **46**, 3187–3189.
57 M. A. Zolfigol, A. Khazaei, A. G. Choghamarani, A. Rostami and M. Hajjami, *Catal. Commun.*, 2006, **7**, 399–402.